JOURNAL LA MULTIAPP

VOL. 05, ISSUE 01 (011-022), 2023
DOI: 10.37899/journallamultiapp.v5i1.782

Neutrinos above the Earth's Surface

Askold Belyakov[1]

[1]*Institute Physics of Earth Russian Academy of Sciences, Moscow, Russia*

**Corresponding Author: Askold Belyakov*
Email: : askbel32@gmail.com

Article Info

Article history:
Received 24 March 2023
Received in revised form 23 Jane 2023
Accepted 12 July 2023

Keywords:
Neutrino
Decay Acoustic Traces
Doppler Effect
Magnetoelastic Geophone
Nyquist Frequency
Borehole
Earth's Surface
Space
Electrical Noise

Abstract

In article "Doppler Effect and neutrino acoustic signatures", published in the journal "LA MULTIAPP" on February 25, 2022, I was forced to touch on an astrophysical topic when, in the data stream obtained by monitoring the acoustic noise of the earth's crust with high amplitude resolution (more 240 dB) and in a wide frequency band (from 0.1 Hz to 50 kHz) events began to appear, the forms and frequencies of which are not typical for geophysics and seismology. Similar forms can be seen in works on the detection of acoustic traces of neutrino decay in water and ice. The possibilities of increasing the sensitivity in measurements in a solid medium are discussed. In addition, underwater and underground facilities are being built that use the effect of Cherenkov radiation. All of these methods require complex and very expensive installations on a huge scale. Even acoustic measurements in water and in wells are very laborious and expensive, and most importantly: such measurements are forever tied to a specific place. Therefore, the creation of a light, compact and mobile device for recording acoustic traces of neutrino decay is an urgent task, the solution of which will allow recording traces of neutrino decay not only in water and the earth's crust, but also in air, into space, on planets and satellites.

Introduction

By a lucky chance, on February 25, 2023 at 18:17:39 I turned on the urban acoustic noise recording system and recorded three files of 30 seconds each. It should be noted here that the computer registration system is installed and always ready for operation. The recording mode is carried out with a sampling frequency of 100 kHz (Nyquist frequency - 50 kHz)! This is the lowest frequency at which it is possible to detect acoustic events associated with the decay of neutrinos, the frequencies of which are in the range from 20 to 50 kHz (zaska et al., 2019; Vandenbroucke et al., 2005; Wolf, 1990). Only the next day I began to analyze the received files and discovered that in the first file there are many acoustic events in the form of bipolar signals, which are sometimes combined into groups of up to tens of events (Belyakov, 2019; Landgrebe, 2003). These events are similar to those previously detected during continuous long-term (2015-2017) monitoring at a depth of 1000 m in the SAFOD well in Parkfield, California. The processing of a digital array of available data (more than 4 TB) would make it possible to establish the order of distribution of astrophysical events of various forms in the annual cycle, but this is laborious, and is not within the scope of the author's interests and competence (Timlelt et al., 2017).

Results and Discussion

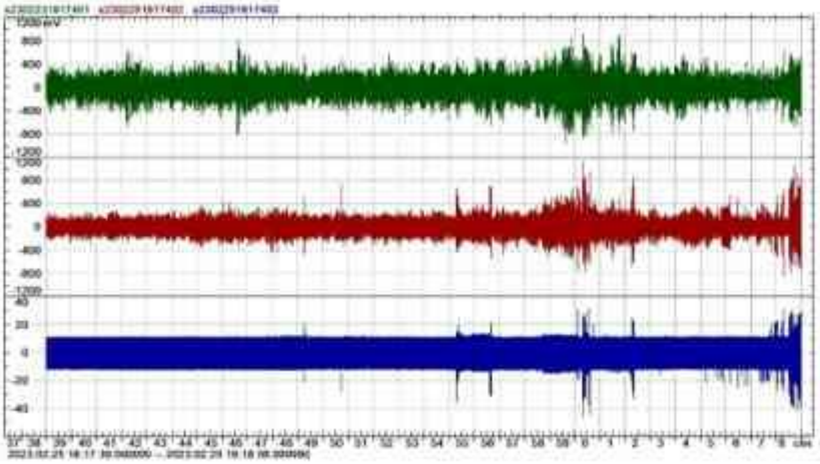

Figure 1. Acoustic tracks in the interval of 30 sec.

In the first file (Fig. 1) there are many bipolar impulses, especially at the end of the file. There are both single and group pulses with a clear Doppler Effect.

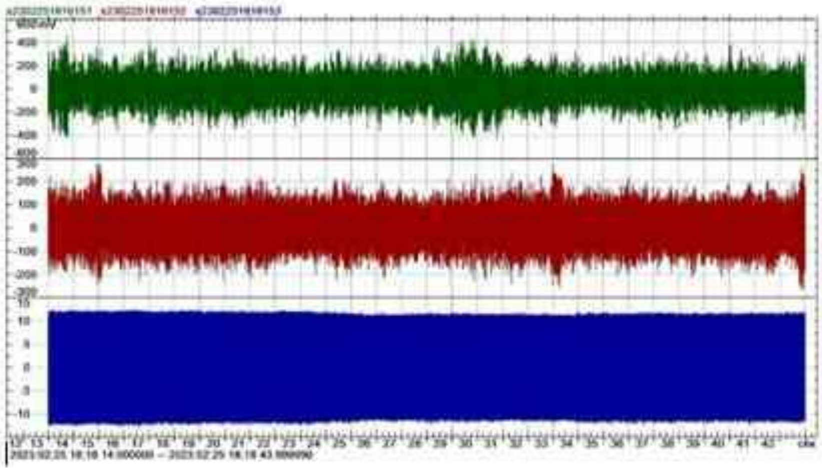

Figure 2. Relatively quiet tracks.

In the second file (Fig. 2), bipolar signals are not massively observed. Basically, electrical noise is recorded there, but sometimes they are very similar to “diamond” phenomena, especially if they are accompanied by the Doppler Effect (Belyakov, 2022).

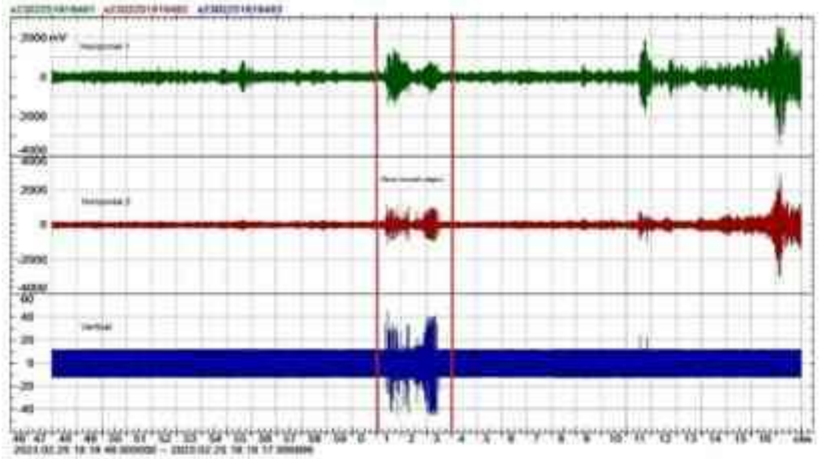

Figure 3. The allocated 30 seconds are eventful.

In the third file (Fig. 3), especially in its middle part, bipolar impulses are observed, mostly combined into close groups.

Acoustic tracks in three directions, shown in Figures 1÷3, were measured by a magnetoelastic inertial geophone with a vector characteristic of three channels - MIG-3V, the sensitivity of which in the operating frequency range exceeds the sensitivity of similar instruments by thousands of times. Due to various force majeure reasons, an open geophone sensor (without a housing) is used. The sensor is attached to the inside wall of the second floor of a wooden house (Fig. 4). The first - the horizontal channel is oriented along the meridian (N-S), the second - along the parallel (E-W), the third - along the vertical. The radiation patterns of all three channels is a volume cosine eight.

Figure 4. Geophone sensor MIG-3V.

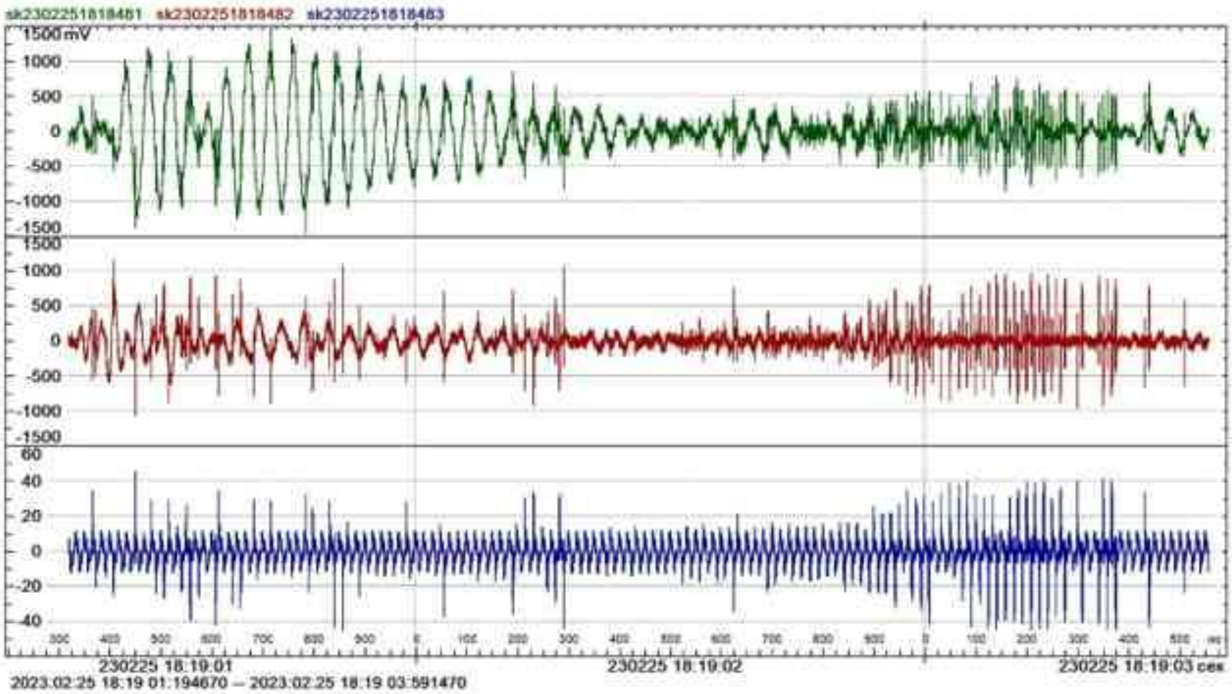

Figure 5. Three-second snippet.

On fig. 5 shows the fragment highlighted in fig. 3 with two red lines. It is characterized by a large number of acoustic traces (bipolar pulses) of high frequency, which are concentrated mainly in its right side (Fig. 8). In the left and middle parts (Fig. 6, 7), the pulse density is much lower (Belyakov, 2017).

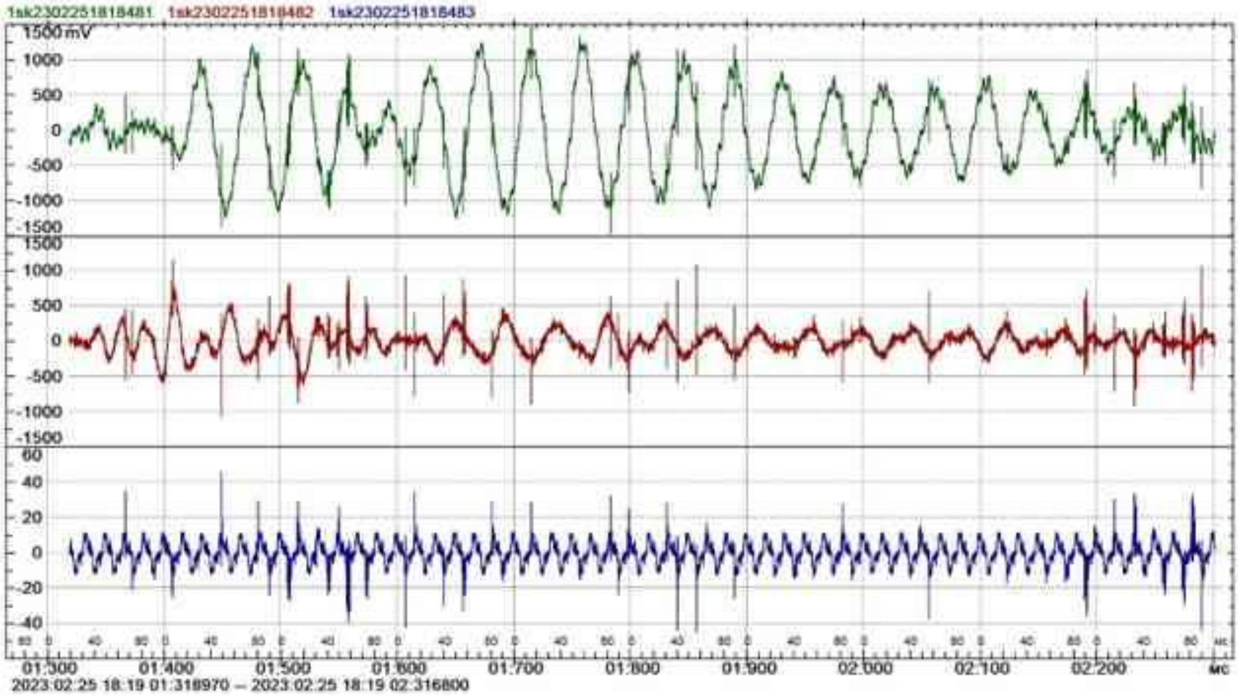

Figure 6. One-second left snippet Figure 5.

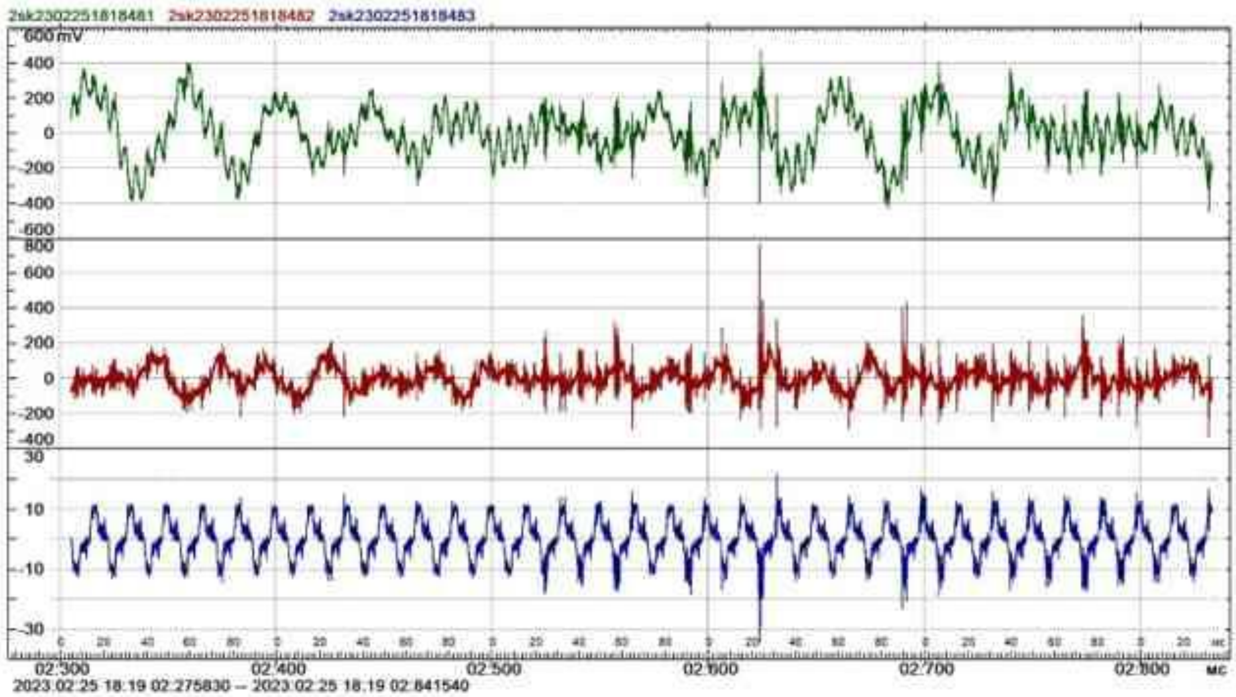

Figure 7. 566 ms snippet central part.

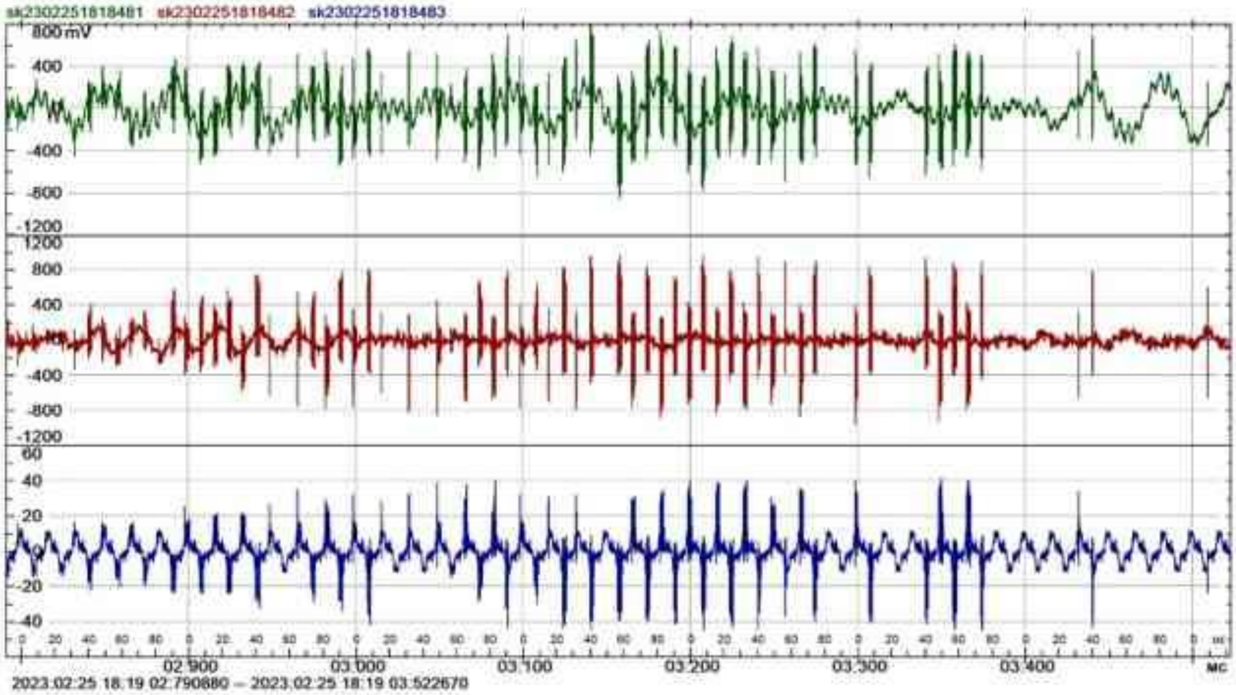

Figure 8. 774 ms snippet right side.

Some doubts are caused by the synchronism of bursts of differently polar pulses with a mains frequency of 60 Hz, which is clearly seen in the vertical channel in Fig. 8. This fact requires additional research.

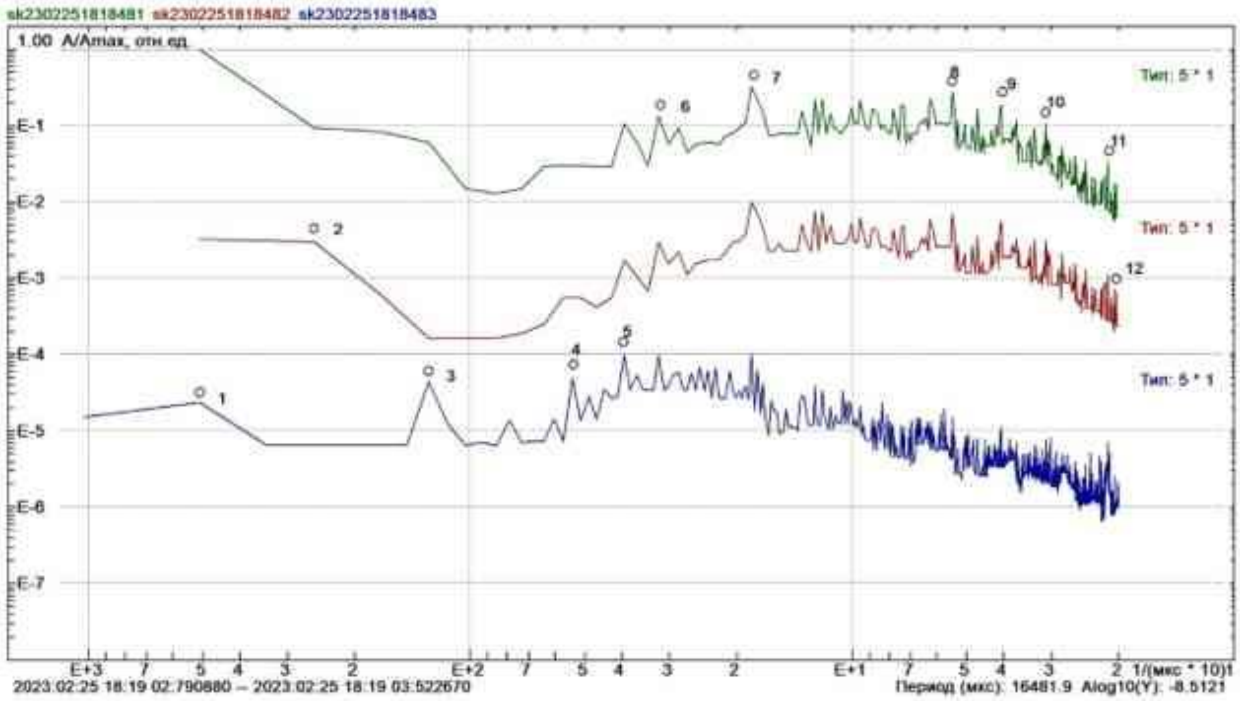

Figure 9. Spectrum snippet right side.

1-200; 2-391; 3-780; 4-1.96; 5-2.54; 6-3.14; 7-5.5; 8-18.3; 9-24.8; 10-32.3; 11-47.6; 12-48.8.

1-3 (Hz), 4-12 (kHz).

Express analysis of the frequency characteristics of the processes can be described by the following figures: the frequency of the bipolar pulse is about 30 kHz, the time interval between pulses in a burst is from 130 to 160 μs; the frequency of the first pulse in a diamond-type event is about 40 kHz. It is difficult to judge the global time interval due to the short observation period.

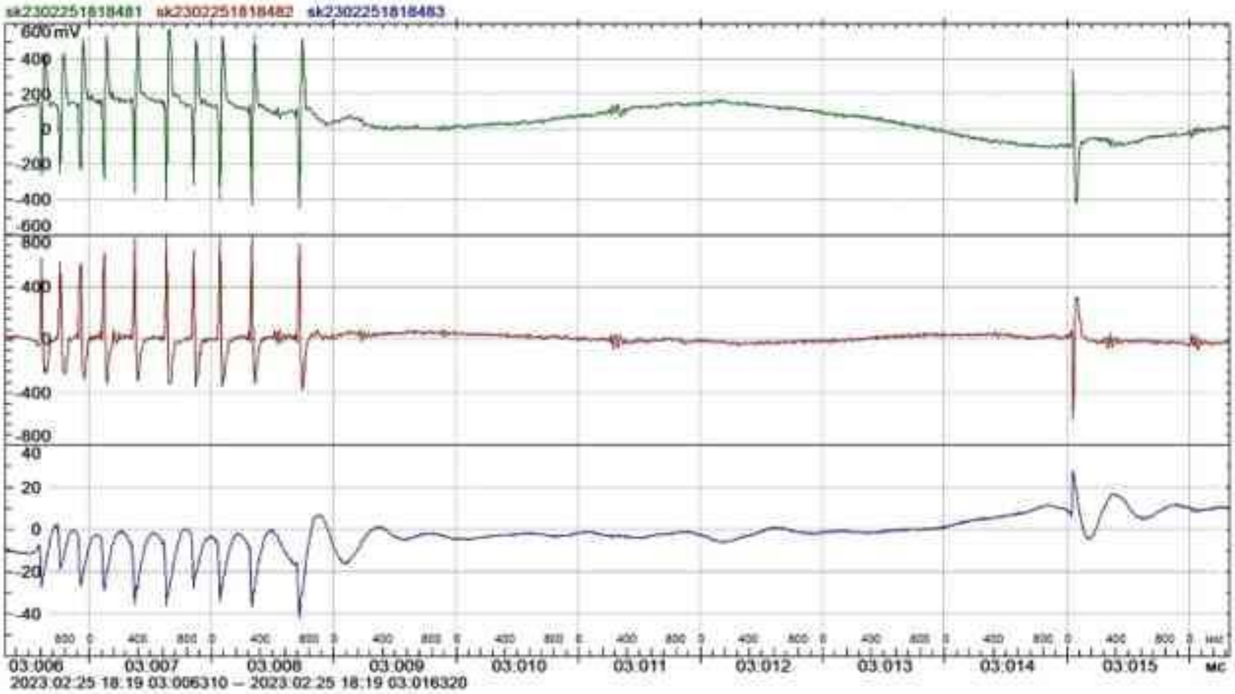

Figure 10. Series of ten bipolar impulse and a single inverted impulse.

In the vertical channel (lower graph in Fig. 10), the Doppler Effect is very clearly visible (Dingle, 1960).

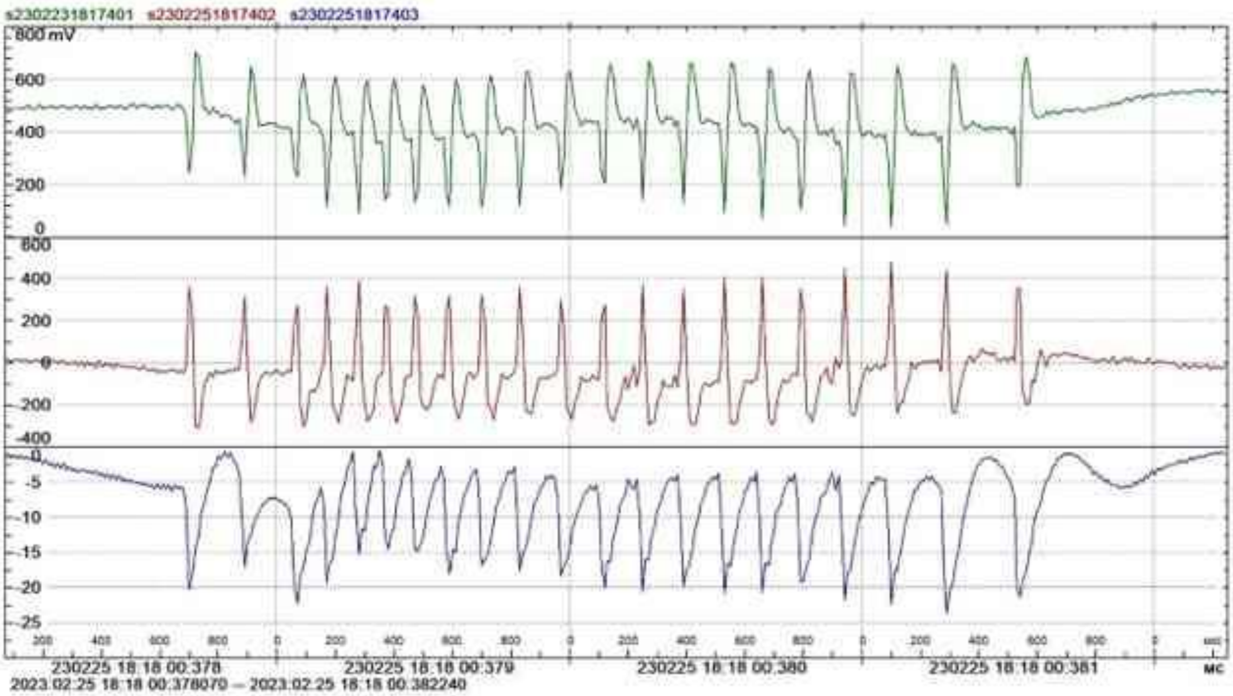

Figure 11. Series of 21 bipolar impulse.

On fig. Figure 11 shows a burst of 21 bipolar pulses extracted from the first file (Figure 1).

ISSN: 2716-3865 (Print), 2721-1290 (Online)

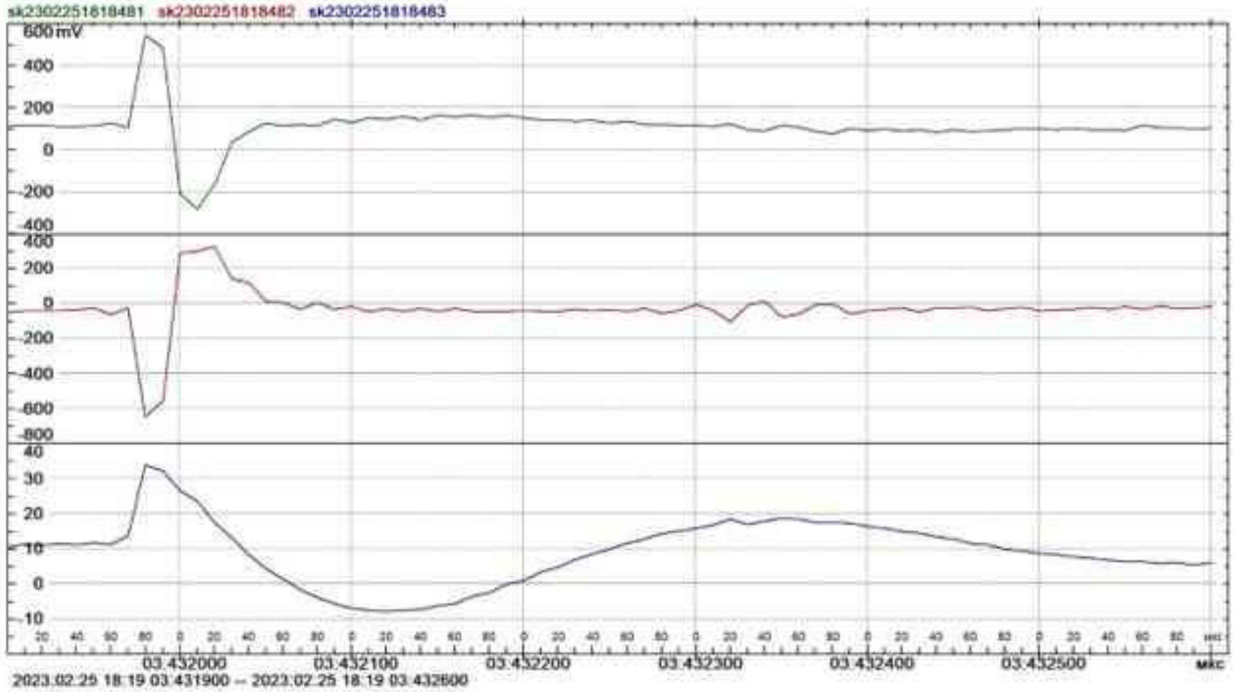

Figure 12. Single bipolar impulse.

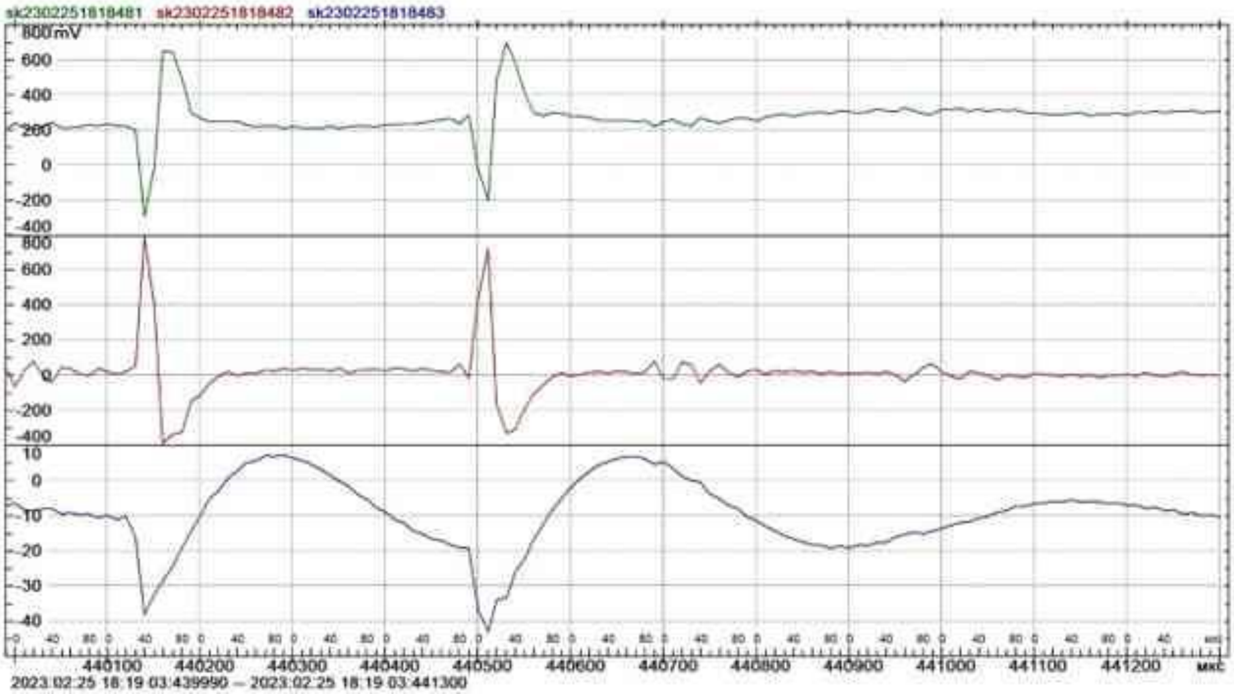

Figure 13. Two bipolar impulse.

ISSN: 2716-3865 (Print), 2721-1290 (Online)

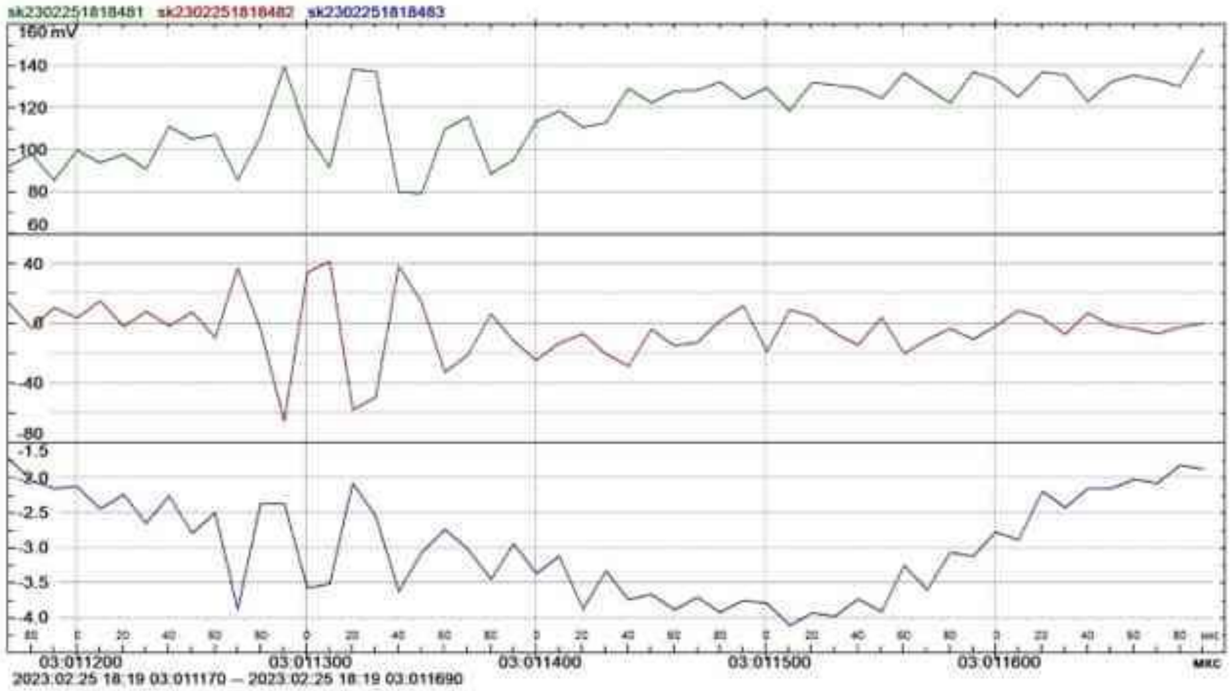

Figure 14. This is the events “diamond”.

Figure 14 clearly shows the Doppler Effect, and the oscillations decay at a time offset of about 100 μs.

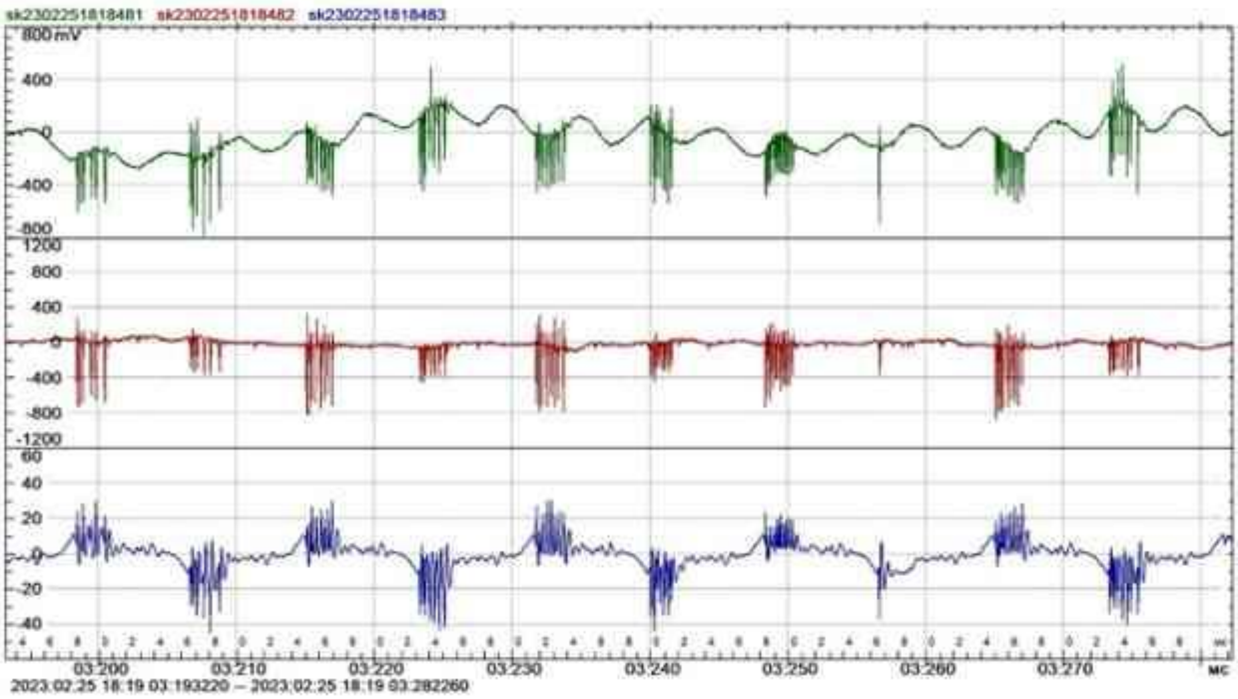

Figure 15. Ten series of bipolar impulse.

ISSN: 2716-3865 (Print), 2721-1290 (Online)

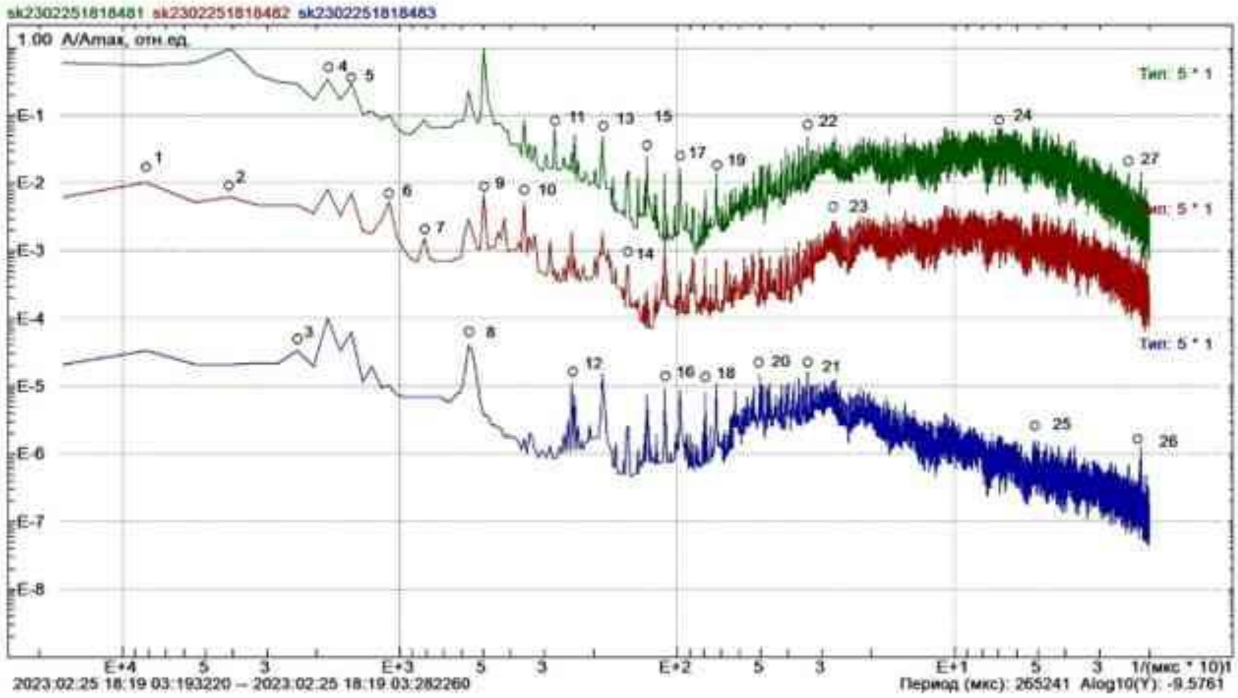

Figure 16. Spectrum ten series of bipolar impulse.

01-12; 02-24; 03-42; 04-56; 05-67; 06-90; 07-120; 08-180; 09-204; 10-286; 11-370; 12-417; 13-540;

14-667; 15-769; 16-909; 17-1.03; 18-1.26; 19-1.39; 20-2.00; 21-2.94; 22-2.94; 23-3.70; 24-14.5;

25-20.0; 26-47.6; 27-43.48 – correspondence of frequencies to points on the spectrum Fig. 16.

Points 01÷16 - Hertz, points 17÷27 - kHz.

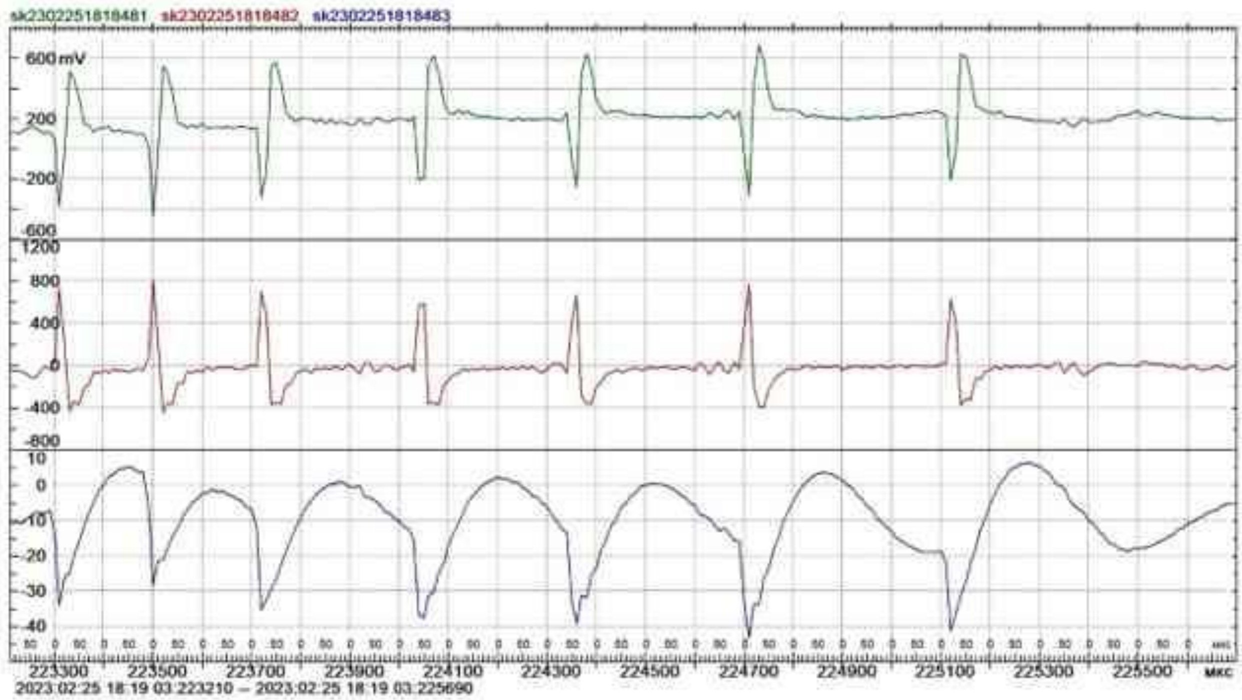

Figure 17. Series of seven bipolar impulse.

ISSN: 2716-3865 (Print), 2721-1290 (Online)

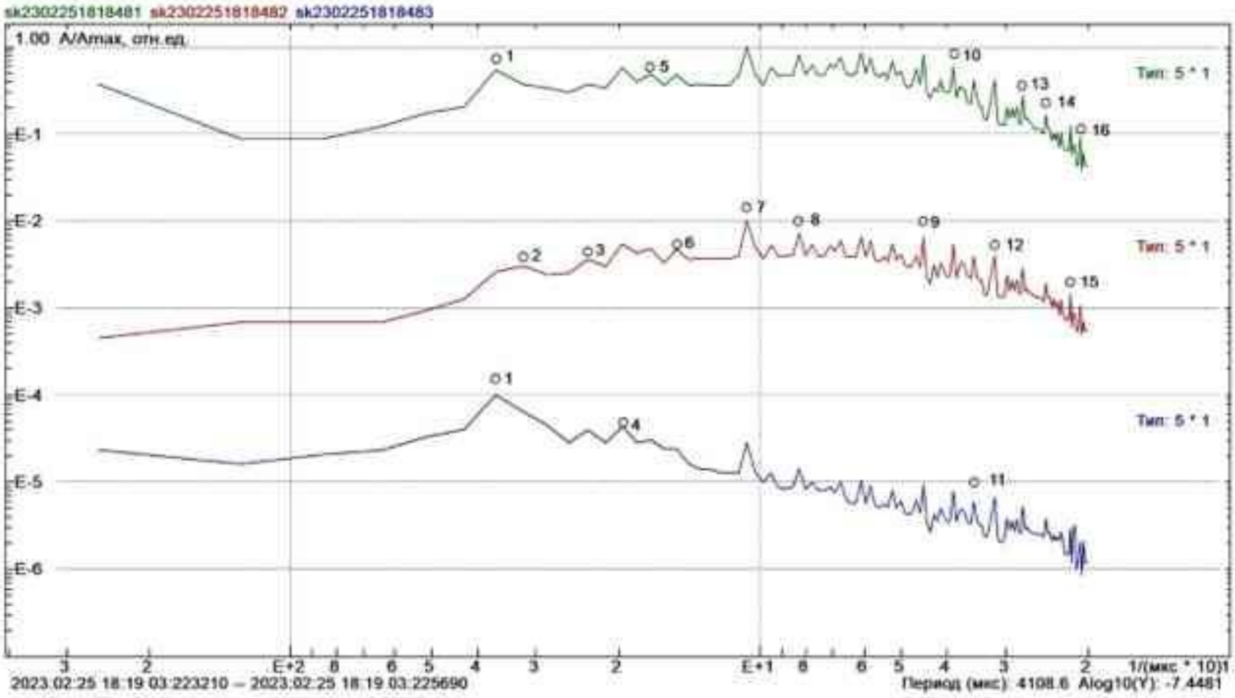

Figure 18. Spectrum series of seven bipolar impulse.

01-2.74; 02-3.18; 03-4.33; 04-5.1; 06-6.67; 07-9.35; 08-12.0; 09-22.4; 10-25.9; 11-28.6; 12-31.7; 13-36.2; 14-40.5; 15-45.9; 16-48.1 – correspondence of frequencies in kHz to points on the spectrum Fig. 18.

I involuntarily remembered the data that were obtained as a result of continuous three years of observation at a depth of 1000 m in the Parkfield rocks in the SAFOD well. Over 4 TB of digital data was received there (Desherevskii et al., 2017). Unfortunately, due to the lack of digital media and taking into account the seismological formulation of the problem, it was decided to record data with a sampling frequency of 10 kHz or a Nyquist frequency of 5 kHz. An example of registering a flow of differently polar impulses in a well is shown in fig. 19.

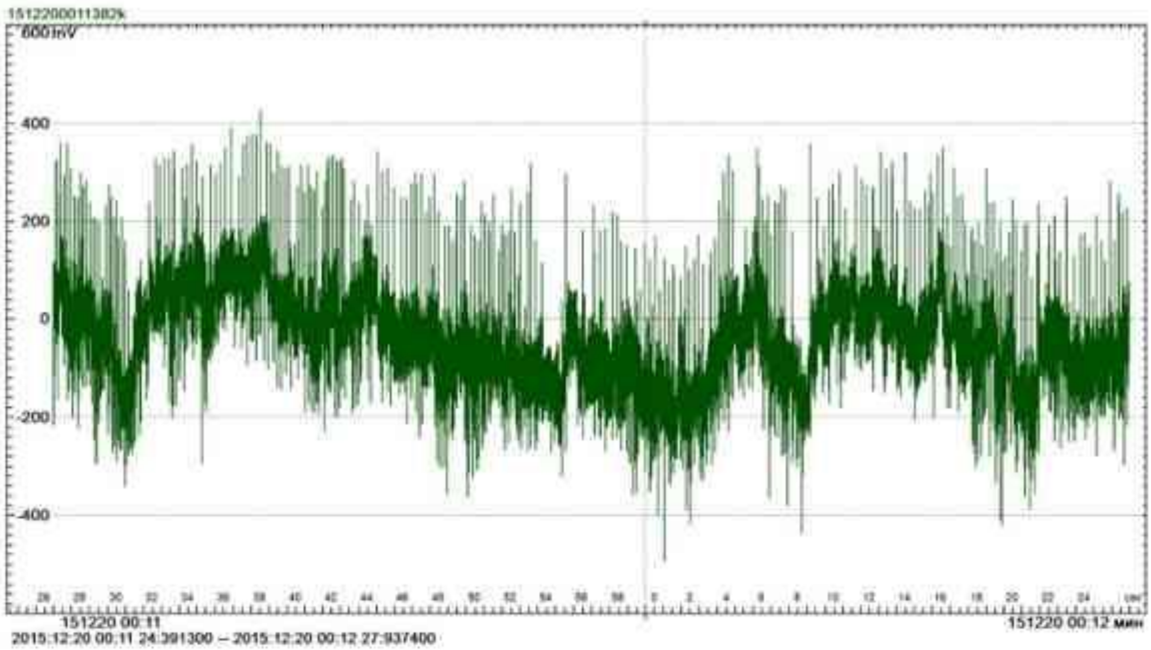

Figure 19. Series of bipolar impulse.

ISSN: 2716-3865 (Print), 2721-1290 (Online)

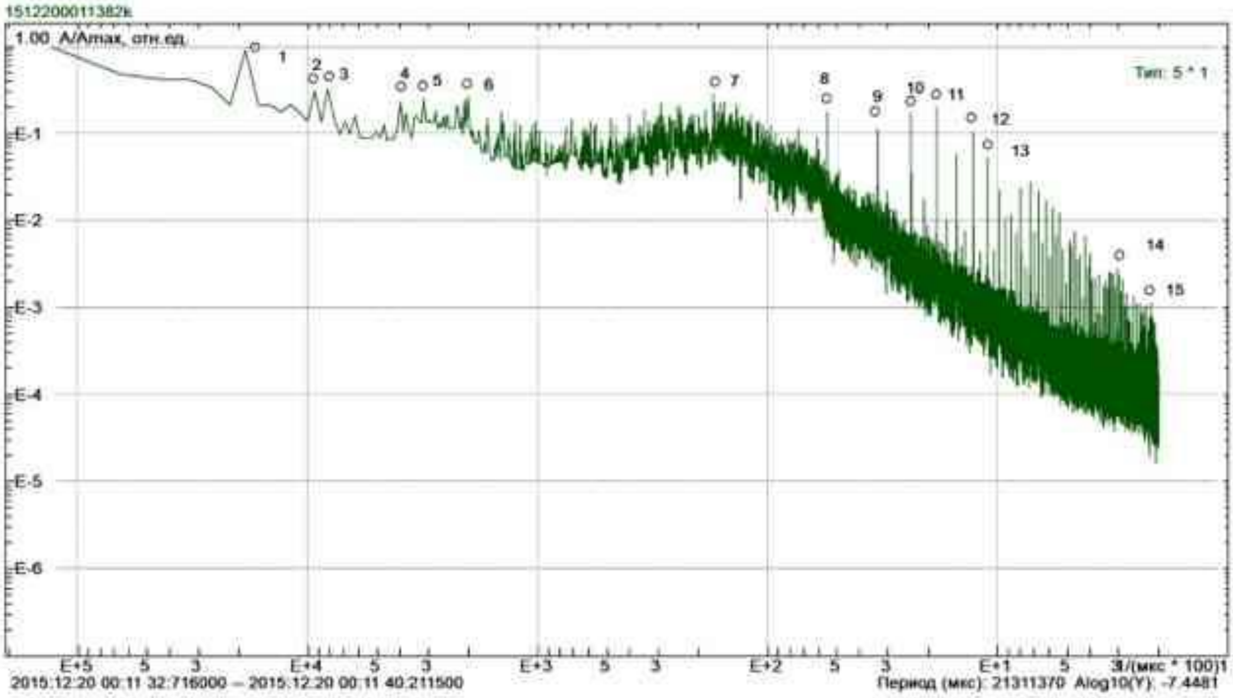

Figure 20. Spectrum series of bipolar impulse.

1-0.5; 2-1.06; 3-1.2; 4-2.5; 4-2.5; 5-3.2; 6-5; 7-58.3; 8-182; 9-301; 10-418; 11-542; 12-786; 13-893; 14-3289; 15-4651 – correspondence of frequencies in Hz to points on the spectrum Fig. 20.

Often, an incorrect choice of the Nyquist frequency leads not only to a multiple distortion of the spectrum frequencies (Fig. 20), but also to a significant distortion of the form of the recorded process, which can be seen in Fig. 21.

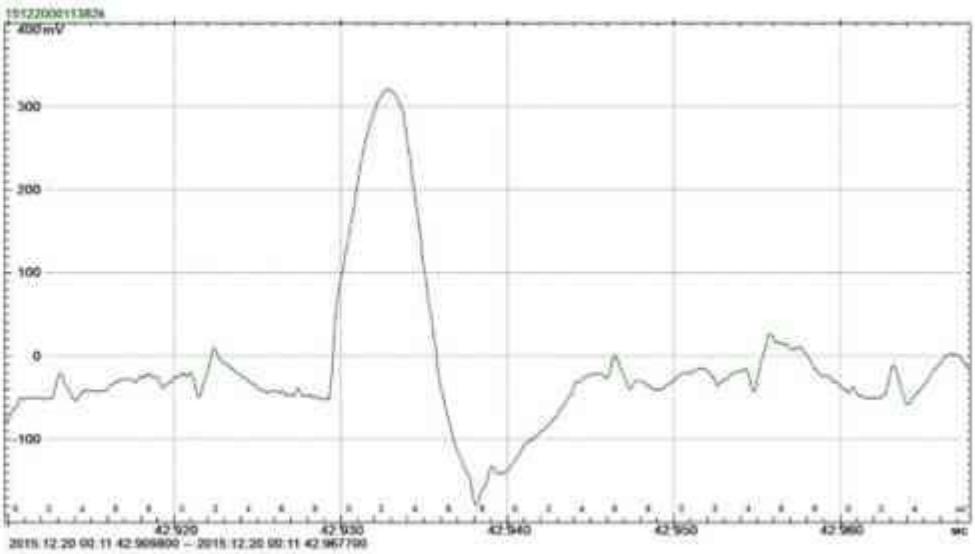

Figure 21. Single distorted bipolar pulse.

Gratitude

I am sincerely grateful to Alexey Desherevsky for his excellent WinABD program and his creative efforts to update it. Without the WinABD program, this and many other works that require transformations, calculations and graphics would not have been possible.

References

Belyakov, A. S. (2022). Doppler Effect and Acoustic Trails of Neutrinos. *Journal La Multiapp*, *3*(1), 1-7.

Belyakov. A. (2017). Acoustic Traces in the Upper Part of the Earth's Crust. *International Journal of Geophysics and Geochemistry 4*(5). 39-50.

Belyakov. A. (2019). Vector measurement of acoustic waves. *LAMBERT Academic Publishing*.

Desherevskii, A. V., Zhuravlev, V. I., Nikolsky, A. N., & Sidorin, A. Y. (2017). Technology for analyzing geophysical time series: Part 2. WinABD—A software package for maintaining and analyzing geophysical monitoring data. *Seismic Instruments*, *53*, 203-223. http://link.springer.com/article/10.3103/S0747923917030021

Dingle, H. (1960). The Doppler Effect and the foundations of physics (i). *The British Journal for the Philosophy of Science*, *11*(41), 11-31.

Landgrebe, D. A. (2003). *Signal theory methods in multispectral remote sensing* (Vol. 24). John Wiley & Sons.

Timlelt, H., Remram, Y., & Belouchrani, A. (2017). Closed-form solution to motion parameter estimation of an acoustic source exploiting Doppler effect. *Digital Signal Processing*, *63*, 35-43.

Trzaska, W. H., Loo, K., Enqvist, T., Joutsenvaara, J., Kuusiniemi, P., & Slupecki, M. (2019). Acoustic detection of neutrinos in bedrock. In *EPJ Web of Conferences* (Vol. 216, p. 04009). EDP Sciences.

Vandenbroucke, J., Gratta, G., & Lehtinen, N. (2005). Experimental study of acoustic ultra-high-energy neutrino detection. *The Astrophysical Journal*, *621*(1), 301.

Wolf, T. G. (1990). *Remote sensing of ionospheric effects associated with lightning using very low frequency radio signals* (Doctoral dissertation, Stanford University).

ISSN: 2716-3865 (Print), 2721-1290 (Online)